



# A Real-Time Algorithm for PPG Signal Processing During Intense Physical Activity

Andrea Gentili<sup>1</sup>(✉), Alberto Belli<sup>1</sup>, Lorenzo Palma<sup>1</sup>, Salih Murat Egi<sup>2</sup>,  
and Paola Pierleoni<sup>1</sup>

<sup>1</sup> Department of Information Engineering (DII), Università Politecnica delle Marche,  
Via Brecce Bianche 12, 60131 Ancona, Italy  
a.gentili@pm.univpm.it

<sup>2</sup> Department of Computer Engineering, Galatasaray University, Istanbul, Turkey

**Abstract.** Photoplethysmography (PPG) is a simple, low cost and non-invasive technique, implemented by pulse-oximeters to measure several clinical parameters, such as heart rate, oxygen saturation ( $SpO_2$ ), respiration and other clinical diseases. Although monitoring of these parameters at rest does not present particular problems, processing PPG signals during intensive physical activity is still a challenge, due to the presence of motion artifacts that affect its true estimation. In our work, a novel time-frequency based algorithm is presented to properly reconstruct PPG signal during intensive physical activity with respect to the ECG signal reference. Starting from raw PPG and acceleration signals, the proposed algorithm initially removes motion artifacts, providing an accurate heart rate estimation. Subsequently, it reconstructs PPG waveform based on both the heart rate information previously computed and the optimal selection of frequency-domain components representing PPG signal. Evaluating our proposed method on a dataset containing signals acquired during high speed running, we found for heart rate estimation an average absolute error of 1.20 BPM and very similar frequency dynamics between the ECG reference and PPG reconstructed HRV time series from a physiological point of view based on visual inspection.

**Keywords:** PPG monitoring · HR estimation · Motion artifacts

## 1 Introduction

Photoplethysmography (PPG) is a simple, low cost and noninvasive technique, implemented by pulse-oximeters, aimed to measure various clinical parameters, such as heart rate (HR), oxygen saturation ( $SpO_2$ ), respiration and other clinical diseases [2]. A pulse oximeter is a small and inexpensive device that measures the changes in arterial blood volume during the cardiac cycle, through the measurement of light-absorption increase due to the systolic increase in arterial blood

volume for  $\text{HbO}_2$  and  $\text{Hb}$ , generally in the red and infrared regions [9]. PPG signal may be recorded from fingertip, ear, forehead or wrist. Thus, it is popular in wearable devices such as smart watches or wristbands to measure heart rate in real time [16] also allowing remote monitoring of physiological parameters through web technologies [12]. There are many promising applications for PPG monitoring, although currently they are mainly used on patients at rest, because PPG signal acquired, especially from wrist, is vulnerable to motion artifact (MA) [7]. The amount of MA added depends on the type of physical exercise and hand movement, or many other anomalies, including shifts in light coupling between tissue and sensor, mechanical pulsation of arterial blood irregular with true pulse rate and increase in sensor touch pressure. Thus, MA contamination on PPG signal result in unreliable  $\text{SpO}_2$  and HR estimation, making this last a challenge. Developing a robust HR estimation algorithm for wearable devices capable of properly estimating HR in the presence of severe MA is therefore a challenge, as the common filtering method does not remove MA noise as the frequency spectrum of this noise overlaps with that of the true PPG signal. Several techniques for MA detection and removal have been proposed in the literature. Some methods rely on adaptive filtering that manages accelerometer data for MA removal. In particular, the spectrum-subtraction-based MA reduction technique [3] removes the acceleration data from that of a PPG signal. The application of adaptive noise cancellation (ANC) [13, 19] is a popular technique used to estimate signals corrupted by additional noise or interference, such as MA. The adaptive filter is inherently self-designed through the use of a recursive algorithm that updates the filter parameters. This approach can be used to obtain the desired level of noise rejection, without a prior estimates of the signal or noise. This method requires two inputs: one PPG signal with a distorted signal and a reference noise signal (RNS) with some possible noise correlation to the first source; the latter obtained as a reference input through an acceleration sensor. It is an advantage to use adaptive method for their fast response time and the capability of continuous processing in time-varying conditions. Experimental results showed that this device produced more reliable signals that were stable against motion artifact corruption under typical types of movement, such as the swinging of the arms [10], making this technique probably one of the best candidate for subjects running or walking in the treadmill, other than underwater applications, as HR and  $\text{SpO}_2$  monitoring of dives or subjects during water walking or jogging. Moreover, from the literature, there are not many techniques aimed to compute PPG signal reconstruction and heart rate variability analysis, in presence of high motion artifacts. In this paper, a real-time algorithm based on time-frequency domain is presented to estimate HR and properly reconstruct PPG signal. In order to test the validity of the proposed algorithms, tests were performed on standard signals available in the literature.

## 2 Methods and Materials

The PPG signals acquired from wrist under intense physical activity has several drawbacks such as poor signal quality and MA corruption. We propose an

algorithm that is able to overcome this issue even in the worst conditions. While poor signal quality may be reduced adopting a good pulse oximeter and an suitable filtering method, MA are more difficult to remove. There are mainly three kind of PPG signals, as explained in [1], namely good, bad and worse PPG signal. The first one presents in the spectrum only one peak that represents the true hearth rate. However, this type of PPG signal is not as common when under intense physical exercise as a bad PPG signal. This last contains more than one dominant peak related to true heart rate and MA and its harmonic. Only with an appropriate tracking algorithm can true HR be detected from this type of PPG signal by removing MA. Ultimately, estimating heart rate can be daunting for the worst PPG signal where MA's harmonic peak position is very close to real HR. Availability of these different kind of PPG signals represents a critical aspects in algorithms development for MA reduction. Therefore in this work it is decided to use an online dataset representative of the various case studies. The dataset used in this study [21] is the most used from literature for testing and developing HR estimation algorithms from PPG signals in presence of motion artifacts [11]. The data recorded in the dataset contains two-channel PPG signals and acceleration signals, other than a one-channel ECG signal, recorded simultaneously from subjects, all sampled at 125 Hz. For each subject, the PPG signals were acquired from wrist by two pulse oximeters with the same green LEDs ( $\lambda = 609$  nm), whose mutual distance is 2 cm, while the acceleration signals were acquired from a three-axis accelerometer. Both of them are embedded in a wrist-band. The ECG signal was recorded at the same time from the chest of each subject using an ECG sensor. Ground truth values of HR are also available, as reference HR, for comparison in this study. The data of the dataset were acquired from 12 healthy male subjects of age 18–35 years. During the registration process, the subjects walked or ran on a treadmill with a variable speed ranging from 6–8 km/h to 12–15 km/h, each data with an approximate duration of 5 min. The provided dataset was used according to the following ground rules for the detection of heart rate from the PPG signal. The heart rate must be calculated from a time window of eight seconds overlapping six seconds from the previous window, also using the previous data up to the current window, but no operations such as moving average filtering or modifying past heart rate estimates based on the current HR estimate.

### 3 Algorithm Development and Real-Time Implementation

The main purpose of the present work is the development of an algorithm able to properly reconstruct the PPG signal acquired during intense physical activity. A simple figure to illustrate the whole idea of this paper is shown in Fig. 1. This can only be achieved if an accurate heart rate estimation is available. Therefore, the proposed algorithm is composed of two main parts. The first part regards the estimate of the heart rate while the second part concerns the reconstruction of the PPG signal.

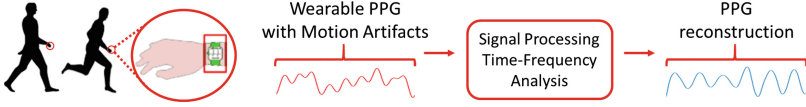


Fig. 1. Simply figure of the proposed algorithm general framework.

### 3.1 HR Estimation

In this work the estimation of the HR is obtained by processing of raw PPG signals ( $p_i$ ) and the accelerometer data ( $a_j(n)$ ).  $a_j(n)$  denotes motion signals recorded from the three-axis accelerometer sensor, where  $n = 0, 1, 2, \dots$  denotes sample index and  $j = x, y, z$  represents axis index.  $p_i$  can be described with a mathematical formulation [15, 18], and modelled as:

$$p_i(n) = d_i(n) + w_i(n) \quad (1)$$

where  $n = 0, 1, 2, \dots$  denotes sample index,  $i = 1, 2$  denotes PPG signal index,  $d_i$  and  $w_i$  represent motion free PPG signal and MA signal, respectively.

In order to estimate the heart rate, we perform a band pass filtering operation on PPG and acceleration data aimed to reduce the random noise introduced due to the sensor probing during recording. A robust HR estimation, during motion, using a recursive least-squares (RLS)-based adaptive filtering technique filters [19, 20] and the Sum Slope Function (SSF) [14] with an adaptive threshold scheme from the literature [4]. Finally, we apply a simple peak verification technique to compute the appropriate HR to deal with unexpected estimation of HR. A block diagram of the steps carried out to estimate HR from motion-corrupted PPG signals is shown in Fig. 2 and described in the following.

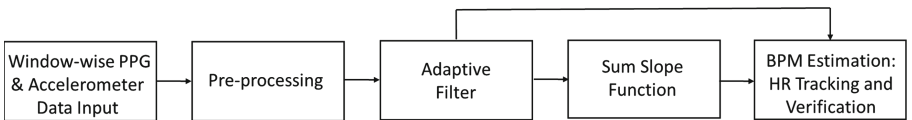
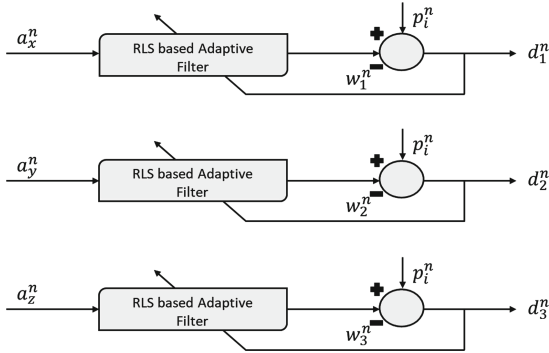


Fig. 2. Block diagram of the proposed method.

**Pre-processing.** In order to remove noise corresponding to the frequencies outside the range of interest [21], a bandpass filter for pulse detection, of band limits 0.4 Hz to 3.5 Hz, on the two PPG signals and three acceleration signals is applied. Subsequently, an energy normalization and average on the two PPG signals to suppress unwanted random noises [17] is applied. Finally, the two raw PPG recorded signals are averaged, clearly showing more reliability detection of the true heart rate position in its spectrum [1].

**Adaptive Filter.** After pre-processing, along with several algorithm proposed in the literature, in order to remove MA still present on PPG signal, we adopted adaptive noise cancellation, that need in input both the PPG signal and a reference noise signal, in our case MA. In [1], studying the relationship between MA and acceleration signals, was shown that the dominant peaks of each channel spectrum clearly represent the MA peak in PPG signal spectrum, unlike the spectrum of vector sum of the three accelerometer axes. Thus, in general, taking any one of the acceleration signals as MA noise reference works well in the most of the cases (see Fig. 3). Passing each one, however, as a MA reference, requires more hardware resources and computational power in separate RLS filters.



**Fig. 3.** Block diagram of the RLS-based MA reduction scheme, respectively, for the three accelerometric signals  $a_x$ ,  $a_y$ ,  $a_z$ .

In this work, we adopted an energy-selective MA reference signal generation from acceleration signals [1]. It is empirically observed that the acceleration signal having greater power band,  $P_{\text{band}}$ , at specific frequency range, usually in the range of 0.5 Hz to 2 Hz, clearly maintains the maximum dominant peaks correlated with the MA peaks in the PPG spectrum. Therefore, the highest power band acceleration signal is chosen as the MA reference signal. To give the best results, the length of the RLS filter is empirically set to 32. The inverse of covariance matrix is initialized as  $10I$ , where  $I$  is identity matrix of order of RLS filter length. Weight vector is initialized to zero. The RLS forgotten factor is set as 0.999. We have experienced that none of these MA three-axis accelerometers reference signals, taken separately, result in accurate enough estimation of HR for each window, where also the combined RNS vector sum of the three accelerometer axes fails in most of the cases too. On the other hand, we empirically observed that sometimes, above all on the first two windows, when the subject is considered almost at rest, in presence of a high random noise, the estimation of HR from periodogram is not accurate. At the same time, trying to reduce MA on PPG signal using only one single RLS filtering stage often fails. Thus, only for the first two windows, a second stage with another RNS is implemented,

in cascade to the first one, improving the signal to noise ratio (N/R) and the accuracy of the HR estimated, only if the difference between the value of the maxima and the second largest  $P_{\text{band}}$  is less than 10%. In addition, as some of the windows are so corrupted with MA that only RLS filter doesn't remove the MA correctly, we adopted a further verification step to track the heart rate in the consecutive PPG windows.

**Sum Slope Function Algorithm.** Heart rate tracking is another key aspect of the proposed method. It results from observation that because the subject on the first two windows is considered at rest, the pulse peaks, in several cases, could be more accurately detected in the time-domain than a spectral tracking, in which the presence of a low signal to noise ratio (S/N) due to random noise can make the HR estimation inaccurate. We chosen to use the Sum Slope Function (SSF) and a peaks finding with adaptive threshold scheme technique [4]. In addition, SSF improves PPG waveform recovery and suppresses the rest of the waveform [22]. The SSF, at time  $i$ ,  $SSF_i$  is defined as:

$$SSF_i = \sum_{k=i-w}^i \Delta x_k \text{ where } \Delta x_k = \begin{cases} \Delta s_k : \Delta s_k > 0 \\ 0 : \Delta s_k \leq 0 \end{cases} \quad (2)$$

where  $w$  and  $s_k$  are the length of the analyzing window and the filtered PPG signal, respectively. In this study, is used the analyzing window size of 0.128 ms for the sampling rate of 125 Hz. Generally, the SSF onset completely coincides with the pulse onset and the pulse peak is totally appeared in the range between the SSF onset and the SSF offset. The algorithm then locates the SSF onset and the SSF offset first and eventually determines the pulse peak within the range as the local limit. Then an adaptive threshold with the SSF and a simple signal conditioning scheme are used to set a search interval for subsequent pulse peak detection by choosing the maximum peak within the search range for a more reliable pulse peak detection. Lastly, overdetected and skipped pulse peaks are deleted and reassessed using knowledge-based rules [6].

**Heart Rate Tracking and Verification.** Thus, for the first two windows, we used both the SSF and RLS method to better estimate the current HR peak. For the other windows, the heart rate is computed only based on spectral analysis of both RLS filtered PPG and pre-processed PPG signal.

1. HR Estimation for Initial Windows: it is necessary pay a particular attention in the measurement of the first HR windows, because the peaks tracking of the next windows depends on the accuracy of the initial estimate, thus accurate estimation in this step improves the subsequent results. For the first window, if the difference between the current estimated HR with both RLS and SSF method is lower than a fixed value, chosen as 4, ( $BPM_{\text{est(SSF)}} - BPM_{\text{est(RLS)}} < 4$ ), the HR of the current window,  $BPM_{\text{est}}$ , is computed as the average of the two above ( $BPM_{\text{est}} = 0.50BPM_{\text{est(SSF)}} +$

$0.50BPM_{\text{est(RLS)}}$ ). Otherwise, if the  $P_{\text{band}}$  of the reference MA acceleration signal is lower than a fixed threshold,  $P_{\text{th}}$ , ( $P_{\text{band}} < P_{\text{th}}$ ), empirically chosen below which the PPG signal is considered free from MA, the HR of the current window is computed by taking the highest dominant peak location in the RLS-processed PPG signal spectrum ( $BPM_{\text{est}} = BPM_{\text{est(RLS)}}$ ), otherwise, taking that estimated with SSF method ( $BPM_{\text{est}} = BPM_{\text{est(SSF)}}$ ). For the second window, if the difference between the estimated HR with both RLS and SSF method is lower than a fixed value, chosen as 4, ( $BPM_{\text{est(SSF)}} - BPM_{\text{est(RLS)}} < 4$ ), the HR of the current window is computed as the average of the estimated HR with both RLS and SSF method, as above. Otherwise, it simply retain the previous estimate for the current window.

2. Peaks Selection: for the other windows, the current HR is computed, in the most of the windows, finding the maxima dominant peak and the associated location in RLS filtered PPG spectrum. However, may occur cases in which RLS fails to remove MA from PPG signal, because MA is too dominant in the PPG or MA peaks position are too close to heart rate peak location to distinguish them. For this purpose, we set a restricted search range for the current HR peak location, reduced to a specific interval, because the differences between hearts rates of consecutive time windows remains within a small range (due to the biological nature of the signal and the overlapping nature of the windows). Hence, the search interval, for the maximum value dominant peak, was set experimentally as  $[R_0 = f_0 - \Delta_R, \dots, f_0 + \Delta_R]$ , where  $f_0$  is the peak location of the estimated HR of the previous window. From this search range, the highest dominant frequency location is obtained,  $f_{\text{curr}}$  and from which  $BPM$  is computed as:

$$\widehat{BPM}_{\text{est}} = \frac{f_{\text{curr}} - 1}{N_{\text{FFT}}} \times 60 \times F_s \quad (3)$$

where  $\Delta_s$  is set to 6.  $N_{\text{FFT}}$  is the number of FFT points used for computing spectrum, set to 3000, and  $F_s$  is the sampling frequency. Next, a second check is needed on the current estimated peak position, before continuing to further verification steps. Only if the distance between the estimated current HR value, from the maxima dominant peak on the pre-processed PPG signal,  $BPM_{\text{pre-processed}}$ , and the previously estimated one,  $BPM_{\text{est(prev)}}$ , is less than the distance between the current HR identified from the RLS filtered PPG signal,  $\widehat{BPM}_{\text{est}}$ , and that previously estimated, and the corresponding frequency peak in the pre-processed PPG signal spectrum,  $f_{\text{pre-processed}}$ , is not on reference signal, ( $f_{\text{acc}}, |(BPM_{\text{pre-processed}} - BPM_{\text{est(prev)}})| < |\widehat{BPM}_{\text{est}} - BPM_{\text{est(prev)}}| \wedge f_{\text{pre-processed}} \neq f_{\text{acc}}$ ), we took  $BPM_{\text{pre-processed}}$  as a value for the current HR peak, ( $\widehat{BPM}_{\text{est}} = BPM_{\text{pre-processed}}$ ).

Otherwise, if the current peak position estimated from the RLS filtered PPG signal is also identified on the reference accelerometric signal and  $P_{\text{band}}$  of the latter is included in certain values experimentally chosen,  $P_{\text{th1}}$  and  $P_{\text{th2}}$  or if the current peak position estimated from the RLS filtered PPG signal do not coincide with that of reference accelerometric signal and the band power of the latter is above the set threshold,  $P_{\text{th2}}$ , ( $f_{\text{cur}} \equiv f_{\text{acc}} \wedge P_{\text{max}} > P_{\text{th1}} \wedge P_{\text{max}} < P_{\text{th2}}$ )  $\vee$  ( $f_{\text{cur}} \neq f_{\text{acc}} \wedge (P_{\text{max}} > P_{\text{th2}})$ ), the current peak of HR is discarded and taken the second highest peak on the PPG signal periodogram. On the other hand, if the power of the accelerometric reference signal experimentally exceeds another set threshold and the maximum peak position on the pre-processed PPG signal corresponds to that from the RLS filtered PPG signal, then we maintain the valid peak as an estimate of the current HR. So, we take the HR identified as the maximum dominant peak estimated from the RLS filtered PPG signal in all the other cases. This is followed by the verification of the current peak according to the following steps: a smooth heart rate tracking and a verifying procedure in order to prevent extremely high or low estimated values of BPM, to prevent from losing tracking over long time [1].

### 3.2 PPG Reconstruction

In order to properly reconstruct PPG signal waveform, a promising time-frequency based approach [5] is adopted, from previous literature [5], based on the optimal selection of frequency-domain components that are believe to represent these PPGs, and not include MA. In addition, to improve the accuracy in the PPG signal reconstruction estimation, over each time window, we used our HR information, previously computed. After that, for each time window, we compared the PPG waveform estimated and the position of the associated peaks, with the reference ECG waveform, provided in the dataset.

The previous algorithm is comprised of 5 steps that are illustrated in Fig. 4. A detailed description of these steps are given below in this subsection.

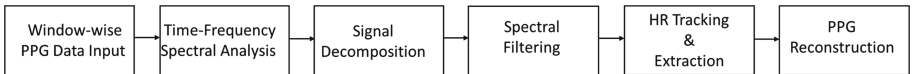


Fig. 4. Block diagram of PPG reconstruction previous algorithm [5].

**Time-Frequency Spectral Analysis.** The PPG pre-processed signal is down-sampled from the previous frequency of 125 Hz to 20 Hz and the variable frequency complex demodulation (VFCDM) based time-frequency spectrum (TFS) is computed.



**Signal Decomposition.** The PPG signal is then decomposed into twelve frequency components, according to the frequency bands in the TFS.

**Spectral Filtering.** Considering HR to be in the range of  $[0.5 \text{ Hz} - 3 \text{ Hz}]$ , which typically contains the true HR, considering both low and high pulse rates, is assumed that the largest two peaks and their corresponding frequencies in the PPG spectrum can provide HR information.

**HR Tracking and Extraction.** If the largest peak is within 10 bpm of the previous HR value, it is chosen; if not, it is checked whether or not the second largest peak is within the 10 bpm range. If the HR value deviates by more than 10 bpm, the HR from the previous window is used.

**PPG Reconstruction.** The PPG signal is then reconstructed, with the summation of VFCDM components, using only the five components within the anticipated HR range, with frequencies closest to the selected HR during each window. Thus, we used the current  $BPM_{est}$ , estimated for each time window, instead of that computed with the previous algorithm, trying to improve the accuracy of the PPG reconstruction (see Fig. 5).

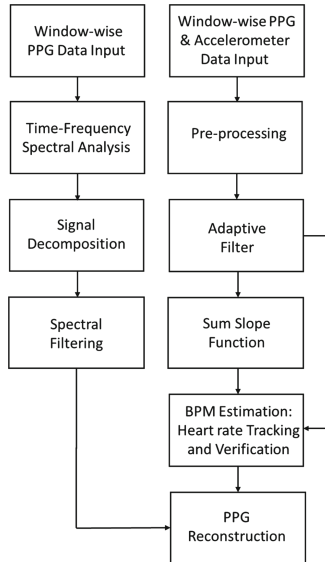


**Fig. 5.** Block diagram of the proposed PPG reconstruction algorithm.

## 4 Results

In this work, an algorithm for PPG signal reconstruction was implemented using HR data previously computed for each time window. In order to evaluate the performance of the proposed algorithm for HR estimation, tests were performed on standard signals of dataset available in the literature [21], comprising also an ECG reference signal acquired simultaneously.

The HR estimation results are presented in terms of Average Absolute Error (AAE), defined as:

$$AAE = \frac{1}{N} \sum_{w=1}^N |BPM_{\text{est}}(w) - BPM_{\text{true}}(w)| \quad (4)$$

where  $BPM_{\text{est}}$  and  $BPM_{\text{true}}$  are estimated and true value of heart rate in BPM of the  $w$ -th window and  $N$  is the total number of time windows. The AAE and its standard deviation value ( $\sigma$ ) is 1.20 and 1.09, respectively. In Figs. 6 and 7 respectively is shown the best and the worst performing subject, respect to their ground truth values, computed from ECG.

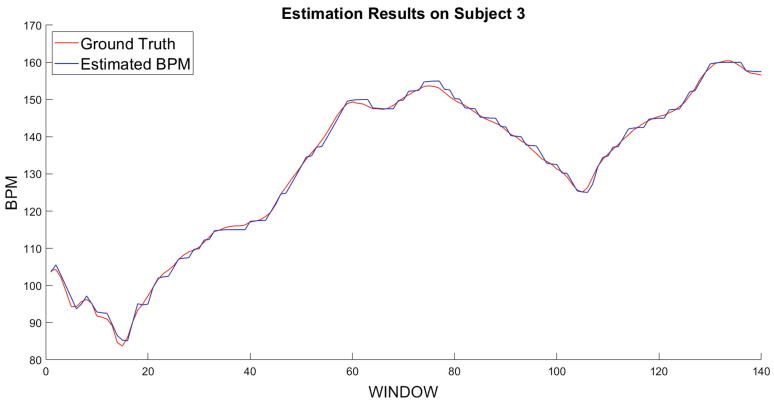


**Fig. 6.** Performance of the proposed method in subject 3 (best subject).

In order to evaluate the performance of the proposed method for HR estimation, two indices are taken into account, such as Pearson correlation ( $r$ ) and Bland-Altman plot. Pearson correlation is a measure of degree of similarity between true and estimated values of heart rate. Higher the value of  $r$ , better

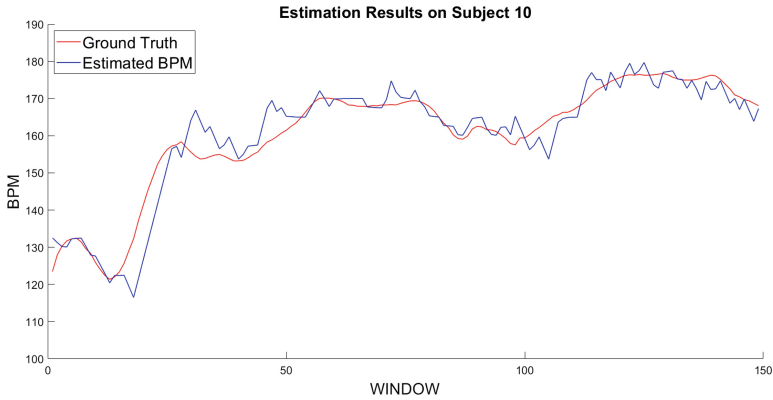


**Fig. 7.** Performance of the proposed method in subject 10 (worst subject).

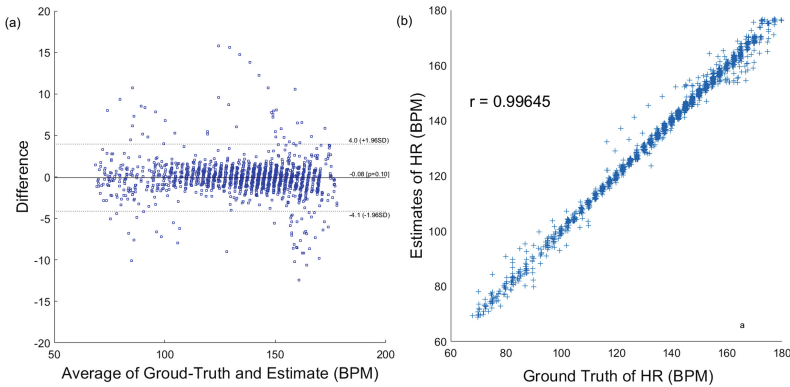


**Fig. 8.** Estimation results on 12 datasets: Blant-Altman plot (a) Pearson Correlation plot (b).

the estimates. The Bland-Altman plot measures the agreement between true and estimates of heart rate. Here limit of agreement (LOA) is computed using the average difference  $\mu$  and the standard deviation  $\sigma$ , which is defined as  $[\mu - 1.96\sigma, \mu + 1.96\sigma]$ . The Pearson correlation coefficient,  $r$ , is found 0.9964 and shown in Fig. 8 (left). Next, Blant-Altman plot is shown in Fig. 8 (right), using all time frames of all 12 subjects. The LOA obtained is  $[-4.1, 4.0]$ .

Both the average absolute error and its standard deviation of HR estimation with our discussed method resulted significantly lower over all 12 subjects (see Table 1). To our knowledge, our algorithm presents very similar accuracy values with respect to the best ones present in the literature, and presenting a lower computational power than most of them.

**Table 1.** Performance comparison in terms of AEE considering all 12 subjects recording.

Subjects	Previous method	Proposed method
Set. 1	$3.65 \pm 2.74$	$1.39 \pm 1.67$
Set. 2	$4.10 \pm 2.86$	$1.28 \pm 1.70$
Set. 3	$4.59 \pm 3.31$	$0.73 \pm 0.54$
Set. 4	$3.78 \pm 2.77$	$1.34 \pm 1.67$
Set. 5	$3.97 \pm 2.95$	$0.82 \pm 1.07$
Set. 6	$3.57 \pm 2.41$	$1.15 \pm 1.42$
Set. 7	$3.70 \pm 2.96$	$0.88 \pm 0.99$
Set. 8	$3.79 \pm 2.67$	$0.86 \pm 0.79$
Set. 9	$4.54 \pm 2.82$	$0.73 \pm 0.50$
Set. 10	$3.43 \pm 2.97$	$3.09 \pm 0.50$
Set. 11	$3.82 \pm 2.20$	$1.42 \pm 1.70$
Set. 12	$4.15 \pm 2.90$	$0.84 \pm 0.61$
Average $\pm$ sd	$3.92 \pm 2.80$	$1.20 \pm 1.09$

Figure 9(a) shows the comparison between pre-processed and PPG reconstructed signal with our method, while Fig. 9(b) shows a zoomed version of the HRV time series obtained from our and the previous method respectively compared with the reference ECG signal concurrently acquired. Physiologically, PPG signal intensity is maximum at the end of diastole, decreasing during systole, when blood is ejected from the left ventricle into the vascular system, hence increasing the peripheral arterial blood volume, as showed in Fig. 10. Thus, from a qualitative point of view, we are able to estimate quite accurate heart rates and it can be observed similar frequency dynamics between the ECG reference and reconstructed HRV time series with our method, better than those obtained with the previous method.

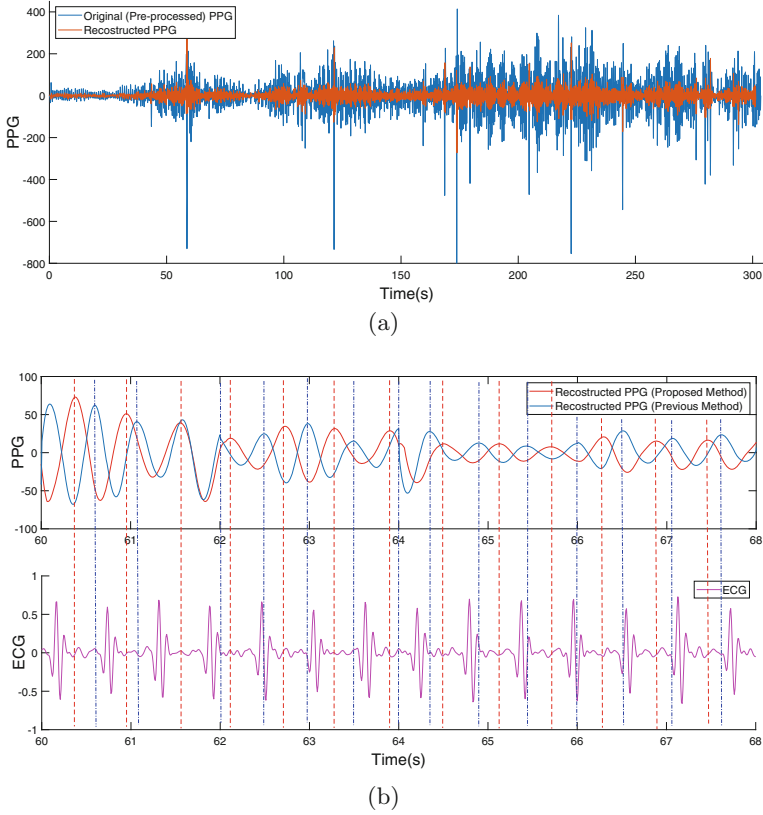


**Fig. 9.** PPG reconstruction (Dataset 1): (a) previous pre-processed and PPG reconstructed signal with the proposed method from the training dataset, (b) Comparison between PPG signal reconstructed with the proposed method and previous method with reference ECG signal.

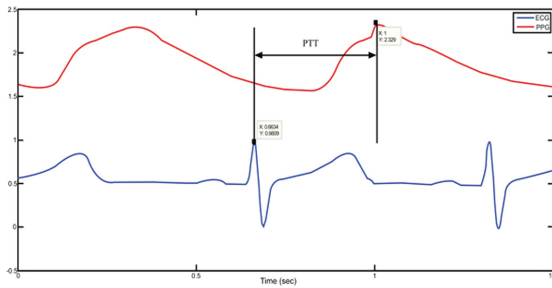


**Fig. 10.** Pulse transit time (PTT), defined as the time interval between the R-peak of ECG and that of PPG within the same cardiac cycle [8].

## 5 Conclusions

In this study, we presented a real-time technique based on time-frequency domain to reduce motion artifacts from PPG signals, taken from an online dataset containing MA, in order to reconstruct the associated waveform on 12 subjects data windows during high speed running. From the results obtained, we are able to estimate quite accurate heart rates, observing similar frequency dynamics between the ECG reference and reconstructed HRV time series. The proposed algorithm may have the potential to compute heart rate variability analysis on the results as well as blood pressure estimation as a clinical aid in the study of cardiovascular diseases. Furthermore, the proposed technique for the reduction of motion artifacts, integrated into a healthcare system, may be used to provide continuous health monitoring without interrupting daily life.

Further studies will be conducted subsequently to improve the proposed technique and obtain quantitative results.

## References

1. Ahamed, S.T., Islam, M.T.: An efficient method for heart rate monitoring using wrist-type photoplethysmographic signals during intensive physical exercise. In: 2016 5th International Conference on Informatics, Electronics and Vision (ICIEV), pp. 863–868. IEEE (2016)
2. Allen, J.: Photoplethysmography and its application in clinical physiological measurement. *Physiol. Meas.* **28**(3), R1 (2007)
3. Fukushima, H., Kawanaka, H., Bhuiyan, M.S., Oguri, K.: Estimating heart rate using wrist-type photoplethysmography and acceleration sensor while running. In: 2012 Annual International Conference of the IEEE Engineering in Medicine and Biology Society, pp. 2901–2904. IEEE (2012)
4. Hahn, M.: An adaptive SSF-based pulse peak detection algorithm for heart rate variability analysis in home healthcare environments. In: International Conference on Ubiquitous Healthcare, pp. 70–71 (2010)
5. Harvey, J., Salehizadeh, S.M., Mendelson, Y., Chon, K.H.: Oxima: a frequency-domain approach to address motion artifacts in photoplethysmograms for improved estimation of arterial oxygen saturation and pulse rate. *IEEE Trans. Biomed. Eng.* **66**(2), 311–318 (2018)
6. Jang, D.G., Farooq, U., Park, S.H., Hahn, M.: A robust method for pulse peak determination in a digital volume pulse waveform with a wandering baseline. *IEEE Trans. Biomed. Circuits Syst.* **8**(5), 729–737 (2014)
7. Jubran, A.: Pulse oximetry. *Crit. Care* **3**(2), R11 (1999)
8. Ma, H.T.: A blood pressure monitoring method for stroke management. *BioMed Res. Int.* **2014**, 1–7 (2014)
9. Nitzan, M., Romem, A., Koppel, R.: Pulse oximetry: fundamentals and technology update. *Med. Devices (Auckl. NZ)* **7**, 231 (2014)
10. Wei, P.: A new wristband wearable sensor using adaptive reduction filter to reduce motion artifact. In: International Conference on Information Technology and Applications in Biomedicine, ITAB 2008. IEEE (2008)
11. Periyasamy, V., Pramanik, M., Ghosh, P.K.: Review on heart-rate estimation from photoplethysmography and accelerometer signals during physical exercise. *J. Indian Inst. Sci.* **97**(3), 313–324 (2017)

12. Pierleoni, P., et al.: An innovative webRTC solution for e-health services. In: 2016 IEEE 18th International Conference on E-health Networking, Applications and Services (Healthcom), pp. 1–6. IEEE (2016)
13. Ram, M.R., Madhav, K.V., Krishna, E.H., Komalla, N.R., Reddy, K.A.: A novel approach for motion artifact reduction in PPG signals based on AS-LMS adaptive filter. *IEEE Trans. Instrum. Meas.* **61**(5), 1445–1457 (2011)
14. Rankawat, S.A., Rankawat, M., Dubey, R.: Heart rate estimation from non-cardiovascular signals using slope sum function and Teager energy. In: 2015 International Conference on Industrial Instrumentation and Control (ICIC), pp. 1534–1539. IEEE (2015)
15. Seyedtabaai, S., Seyedtabaai, L.: Kalman filter based adaptive reduction of motion artifact from photoplethysmographic signal. In: Proceedings of World Academy of Science, Engineering and Technology, vol. 27 (2008)
16. Tamura, T., Maeda, Y., Sekine, M., Yoshida, M.: Wearable photoplethysmographic sensors-past and present. *Electronics* **3**(2), 282–302 (2014)
17. Temko, A.: Estimation of heart rate from photoplethysmography during physical exercise using Wiener filtering and the phase vocoder. In: 2015 37th Annual International Conference of the IEEE Engineering in Medicine and Biology Society (EMBC), pp. 1500–1503. IEEE (2015)
18. Wood, L.B., Asada, H.H.: Low variance adaptive filter for cancelling motion artifact in wearable photoplethysmogram sensor signals. In: 2007 29th Annual International Conference of the IEEE Engineering in Medicine and Biology Society, pp. 652–655. IEEE (2007)
19. Yousefi, R., Nourani, M., Ostadabbas, S., Panahi, I.: A motion-tolerant adaptive algorithm for wearable photoplethysmographic biosensors. *IEEE J. Biomed. Health Inform.* **18**(2), 670–681 (2013)
20. Yousefi, R., Nourani, M., Panahi, I.: Adaptive cancellation of motion artifact in wearable biosensors. In: 2012 Annual International Conference of the IEEE Engineering in Medicine and Biology Society, pp. 2004–2008. IEEE (2012)
21. Zhang, Z., Pi, Z., Liu, B.: TROIKA: a general framework for heart rate monitoring using wrist-type photoplethysmographic signals during intensive physical exercise. *IEEE Trans. Biomed. Eng.* **62**(2), 522–531 (2014)
22. Zong, W., Moody, G., Mark, R.: Reduction of false arterial blood pressure alarms using signal quality assessment and relationships between the electrocardiogram and arterial blood pressure. *Med. Biol. Eng. Comput.* **42**(5), 698–706 (2004)